

Supporting Information

Baek et al. 10.1073/pnas.0805852105

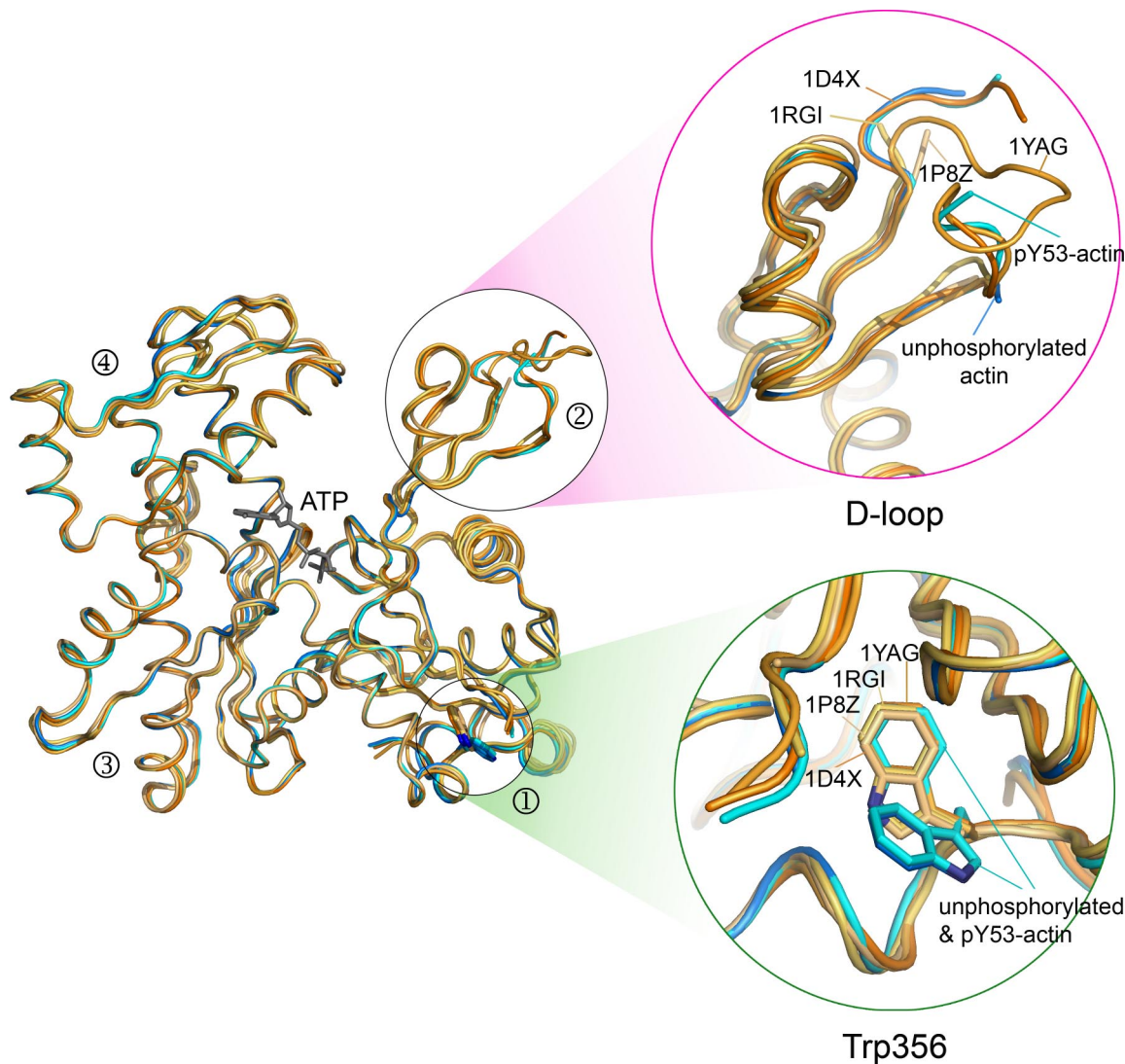


Fig. S1. Gelsolin-actin structures determined under different conditions are very similar. The structures of G1 with unphosphorylated *Dictyostelium* actin and pY53-actin are strikingly similar to each other, and to prior structures of mammalian skeletal α -actin with G1 (1) and gelsolin segments 1–3 (2), as well as *S. cerevisiae*, *C. elegans*, and *Dictyostelium discoideum* actin with G1 (3). The only differences occur in the D-loop (*Upper Inset*) and the orientation of Trp-356 (*Lower Inset*). The D-loop is one of the most flexible parts of the actin molecule, and it is disordered in most of the structures but becomes partially ordered in the structure of pY53-actin (see also [Movie S1](#)). In the structures of gelsolin with unphosphorylated actin and pY53-actin, the region around Trp-356 is flexible and Trp-356 adopts two side-chain orientations. In any other structure of actin, Trp-356 adopts a single and unique rotamer orientation, including in the structure of unphosphorylated actin with profilin determined here (see also [Fig. S5](#)).

1. McLaughlin PJ, Gooch JT, Mannherz HG, Weeds AG (1993) Structure of gelsolin segment 1-actin complex and the mechanism of filament severing. *Nature* 364:685–692.
2. Burtneck LD, Urosev D, Irobi E, Narayan K, Robinson RC (2004) Structure of the N-terminal half of gelsolin bound to actin: Roles in severing, apoptosis and FAF. *EMBO J* 23:2713–2722.
3. Vorobiev S, et al. (2003) The structure of nonvertebrate actin: Implications for the ATP hydrolytic mechanism. *Proc Natl Acad Sci USA* 100:5760–5765.

b 116 203 446 545 602 717 846 917 1045 1132 1260 1416
 D51 - S52 - pY53 - V54 - G55 - D56 - E57 - A58 - Q59 - S60 - K61 - R62
 1435 1320 1232 989 890 833 718 589 528 390 303 175 y

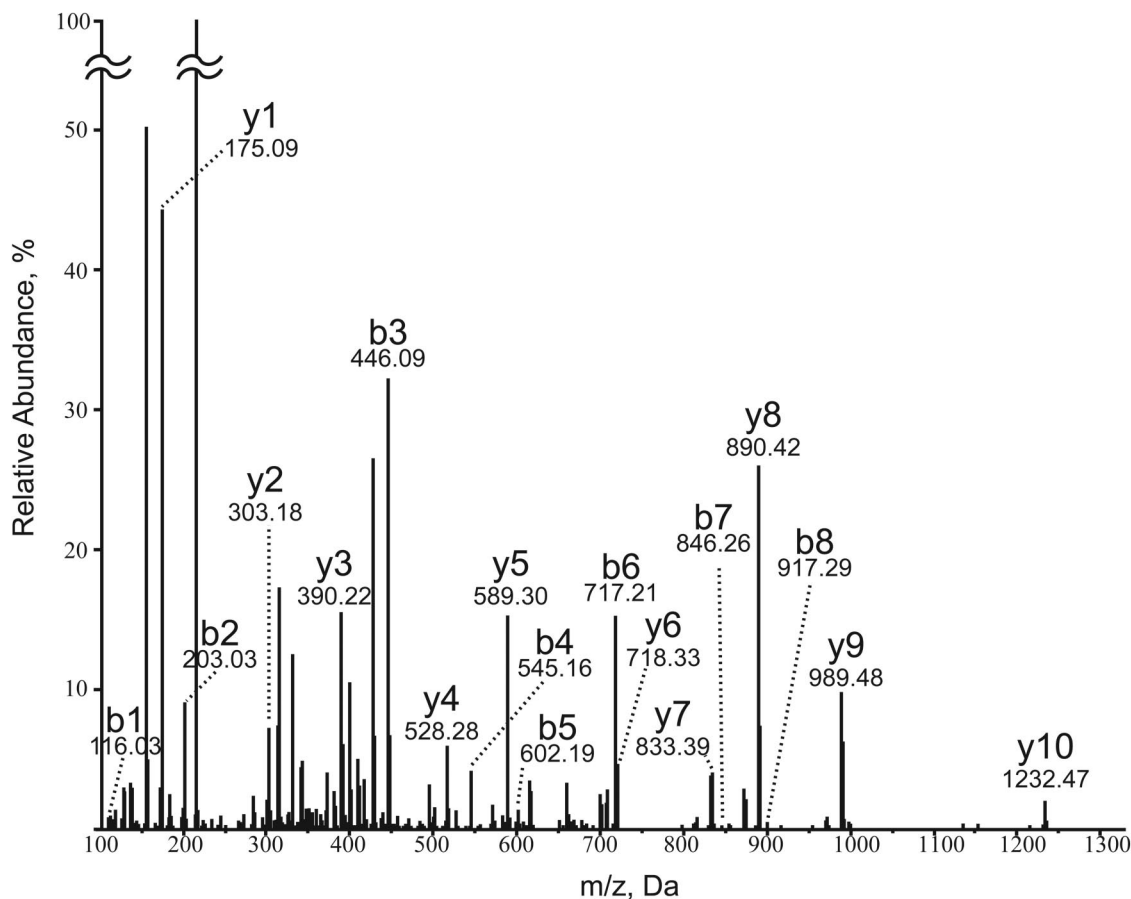


Fig. S2. Tandem mass spectrometry analysis of crystals of G1 with pY53-actin and unphosphorylated actin. Phospho-peptides from tryptic digestions of protein samples obtained from the crystals were separated by metal affinity chromatography and analyzed by tandem mass spectrometry. Phospho-peptides were detected only in samples obtained from crystals of G1-pY53-actin. The masses of various peptide fragments (underlined) correspond to the forward (b) or backward (y) estimates of the theoretical masses of peptides around the phosphorylated Tyr-53.

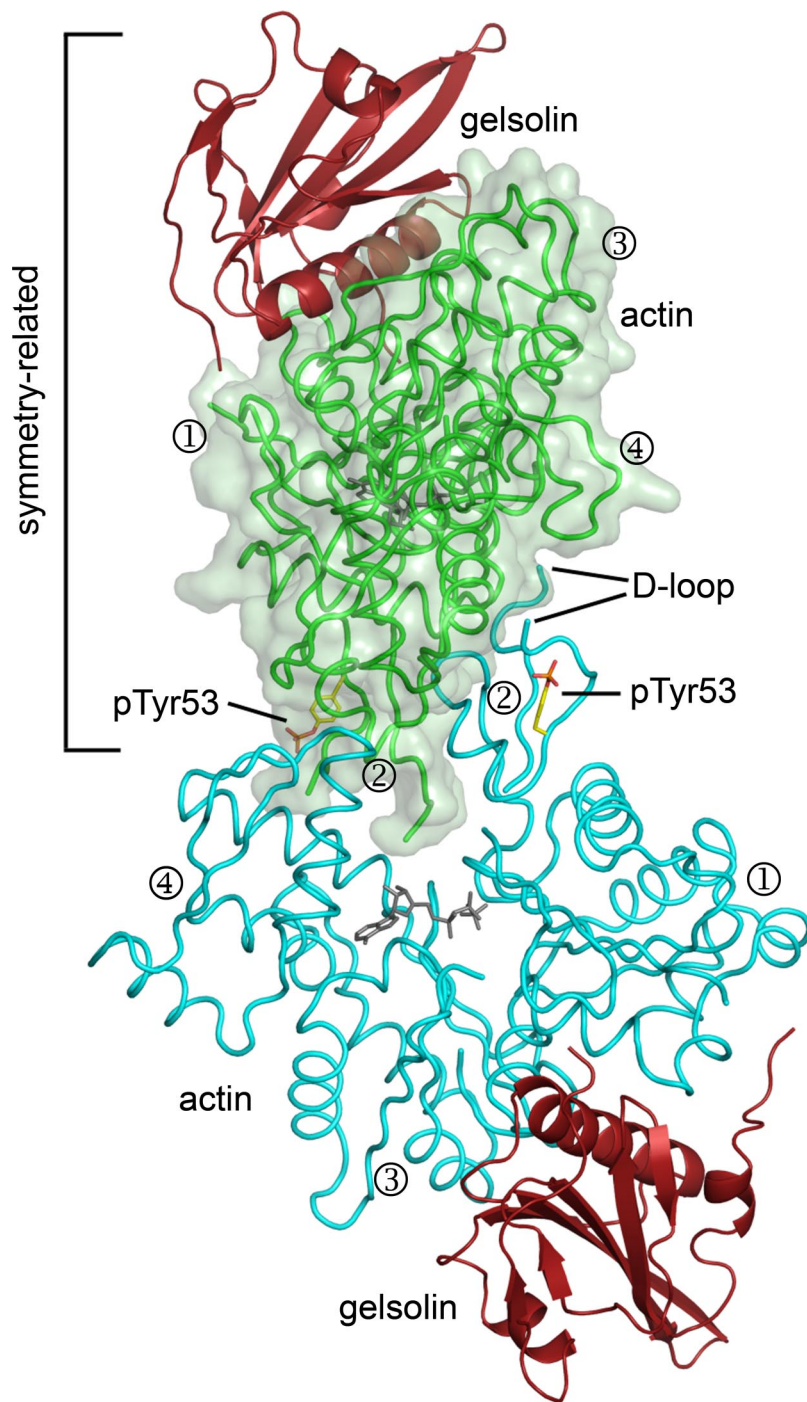


Fig. S3. Two symmetry-related complexes interact head-to-head in the crystals of G1 with unphosphorylated actin and pY53-actin. This crystal packing contact occurs near the D-loop, which might have limited the full extent of the conformation change due to phosphorylation of Tyr-53. The positions of actin subdomains 1–4 are indicated. Color code: actin, blue or green; G1, red.

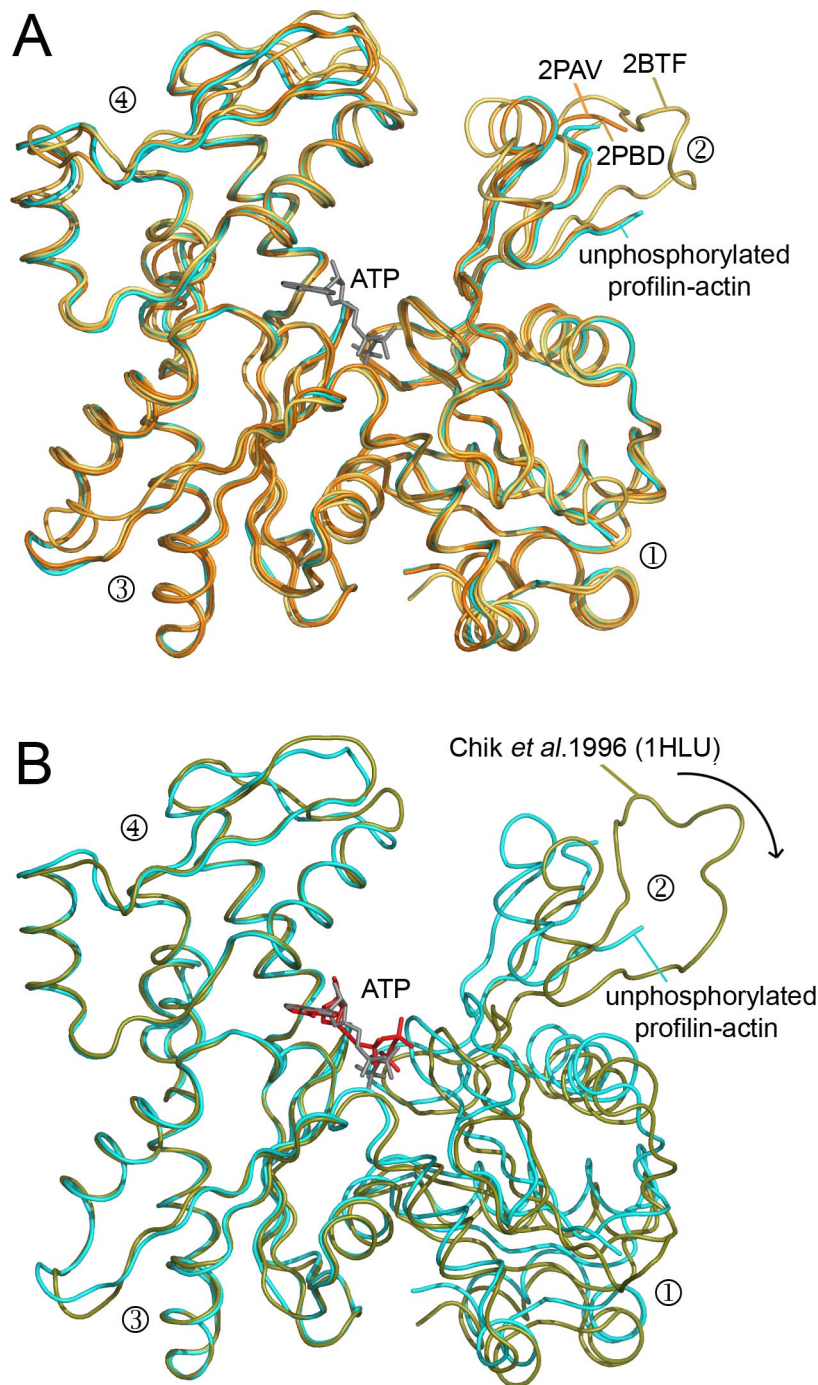


Fig. S4. Comparison of profilin-actin structures. (A) The structure of profilin-*Dictyostelium*-actin is very similar to the original structure of profilin- β -actin (1) and to two structures of profilin- α -actin determined under different conditions (2). In all these structures, the nucleotide cleft is moderately open (Fig. 2A). (B) The notable outlier is the wide-open structure of profilin- β -actin (3) which is far more open than any other actin structure. This structure also presents a distorted molecule of ATP, which is shifted from the canonical position of the nucleotide in other actin structures (red). A similarly wide-open cleft was observed in the structure of nucleotide-free actin-related protein 3 (Arp3), determined as part of the seven-protein Arp2/3 complex (1K8K) (4). Thus, it is possible that the wide-open structure of profilin- β -actin resembles that of nucleotide-free actin, a state that is unstable and has never been crystallized. The positions of actin subdomains 1–4 are indicated.

1. Schutt CE, Myslik JC, Rozycki MD, Goonesekere NC, Lindberg U (1993) The structure of crystalline profilin-beta-actin. *Nature* 365:810–816.
 2. Ferron F, Rebowski G, Lee SH, Dominguez R (2007) Structural basis for the recruitment of profilin-actin complexes during filament elongation by Ena/VASP. *EMBO J* 26:4597–4606.

3. Chik JK, Lindberg U, Schutt CE (1996) The structure of an open state of beta-actin at 2.65 Å resolution. *J Mol Biol* 263:607–623.
 4. Robinson RC, et al. (2001) Crystal structure of Arp2/3 complex. *Science* 294:1679–1684.

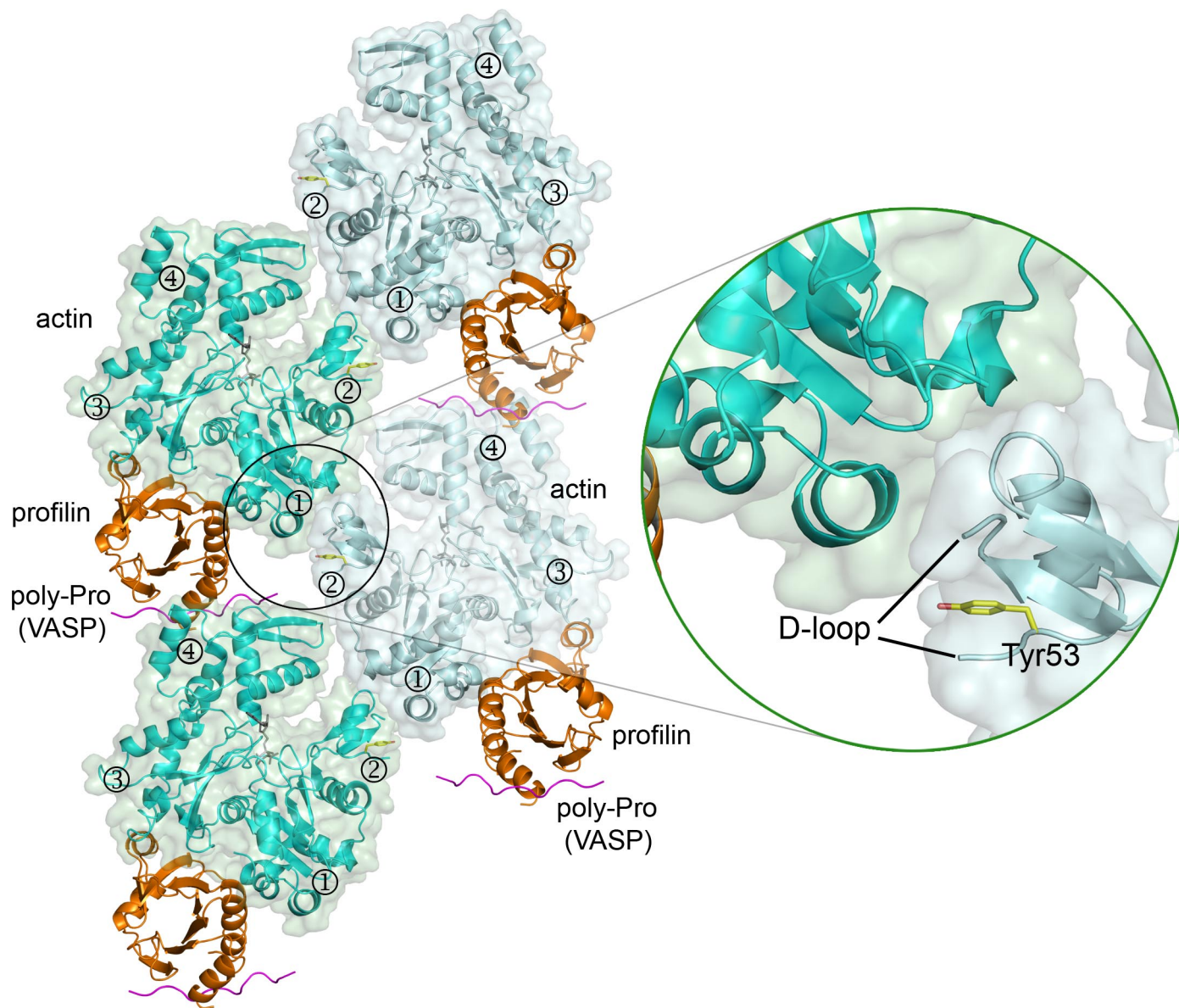
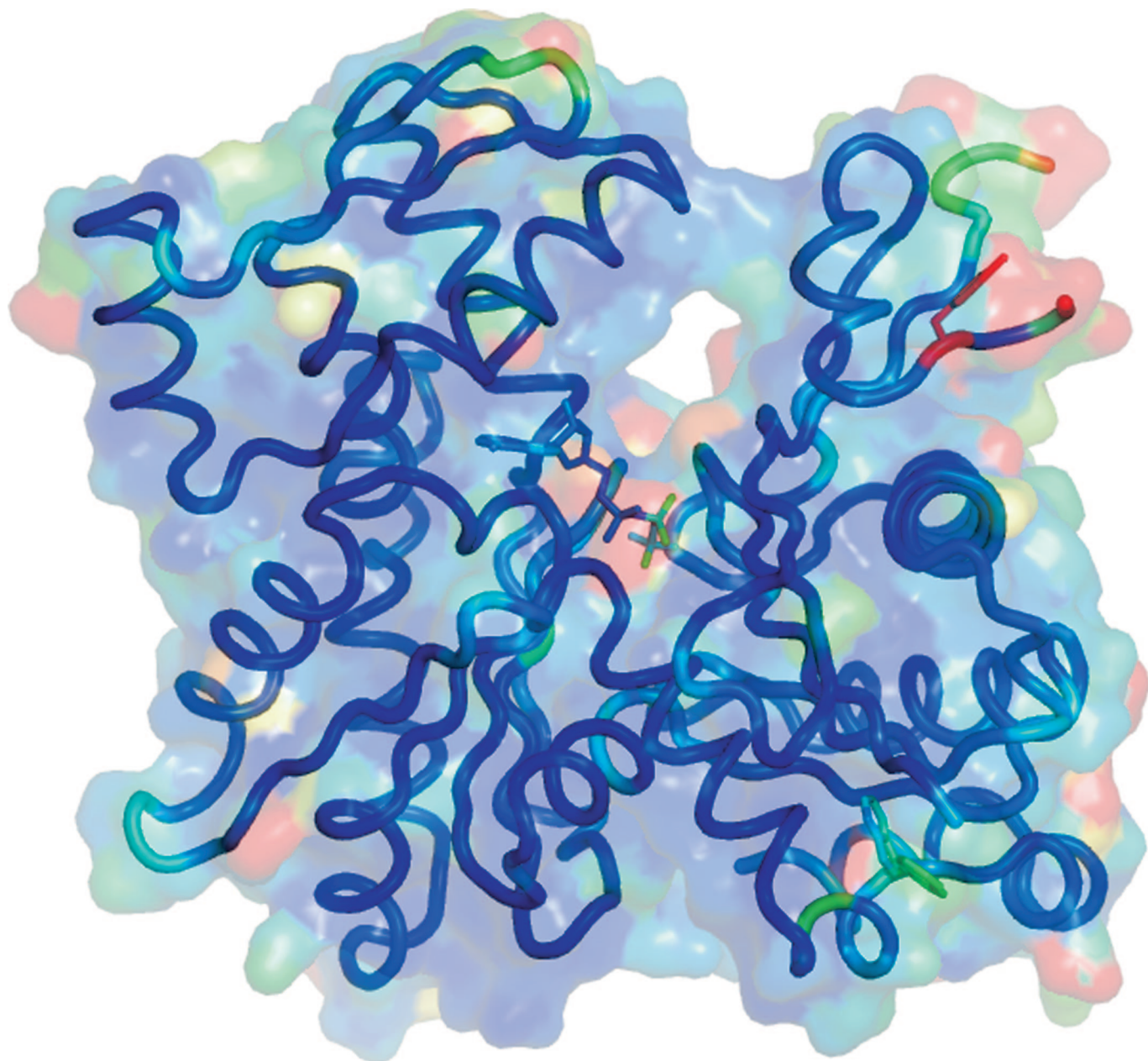
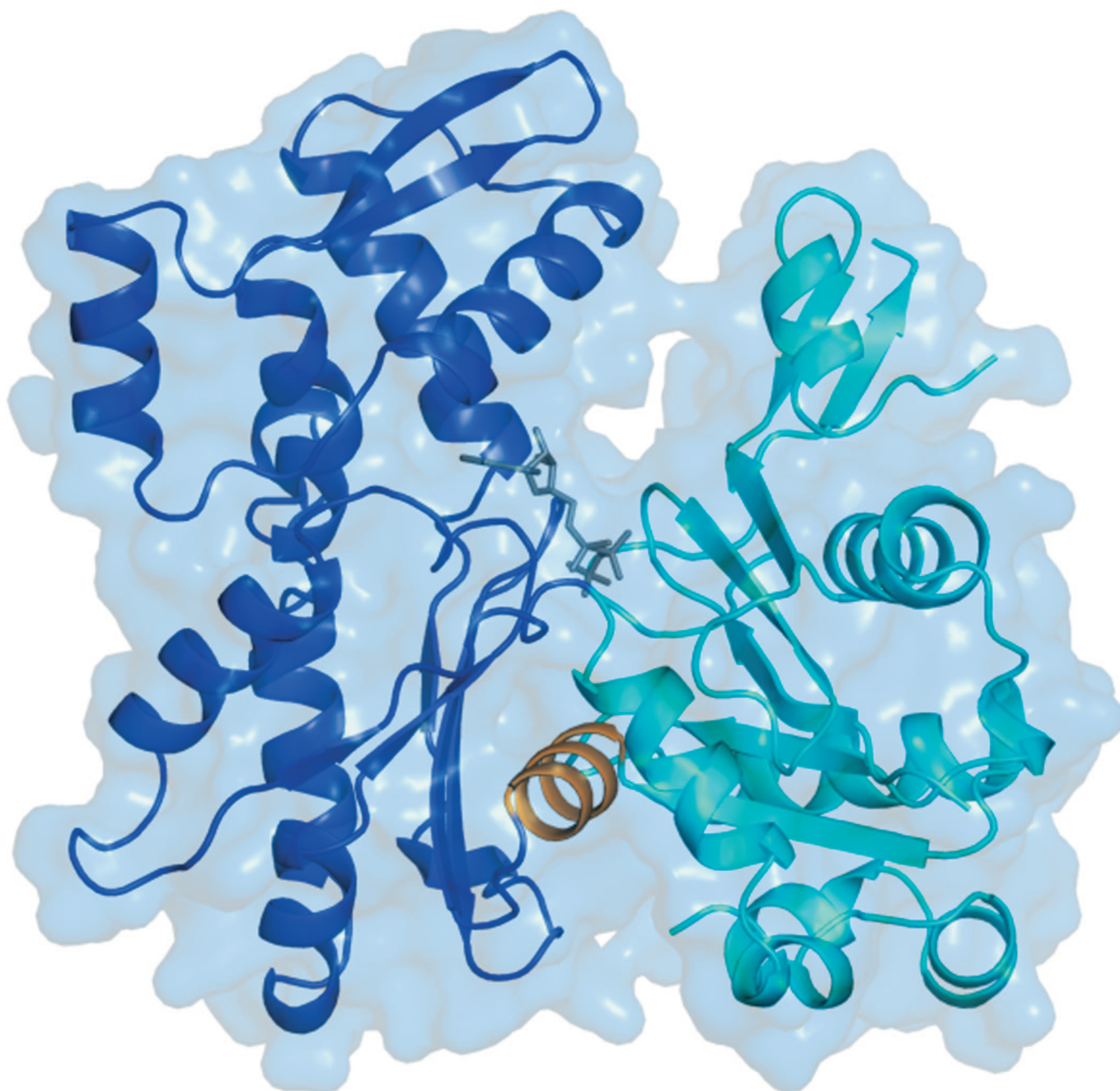


Fig. S6. The D-loop falls near a crystal packing contact in the crystals of profilin with unphosphorylated actin. A phosphorylation-dependent conformational change in the D-loop would be expected to break this crystal packing contact, which may have interfered with the crystallization of the profilin-pY53-actin complex. Color code: actin, cyan or aqua; profilin, gold; VASP polyPro, magenta.



Movie S1. Conformation change upon phosphorylation of Tyr-53 of *Dictyostelium* actin. The movie illustrates a linear interpolation between the atomic coordinates of the complexes of unphosphorylated actin and pY53-actin with gelsolin segment 1 (G1). For clarity, we show only the actin portion of the structures. The C α -trace and transparent surface representations are colored according to displacement, using a color ramp from blue (minimum displacement) to red (maximum displacement). Note that the region around Tyr-53 undergoes maximum displacement. Although other parts of the molecule also appear to move, including the bound nucleotide and Trp-356, smaller displacements fall within the limits of average coordinate errors for these high-resolution structures.

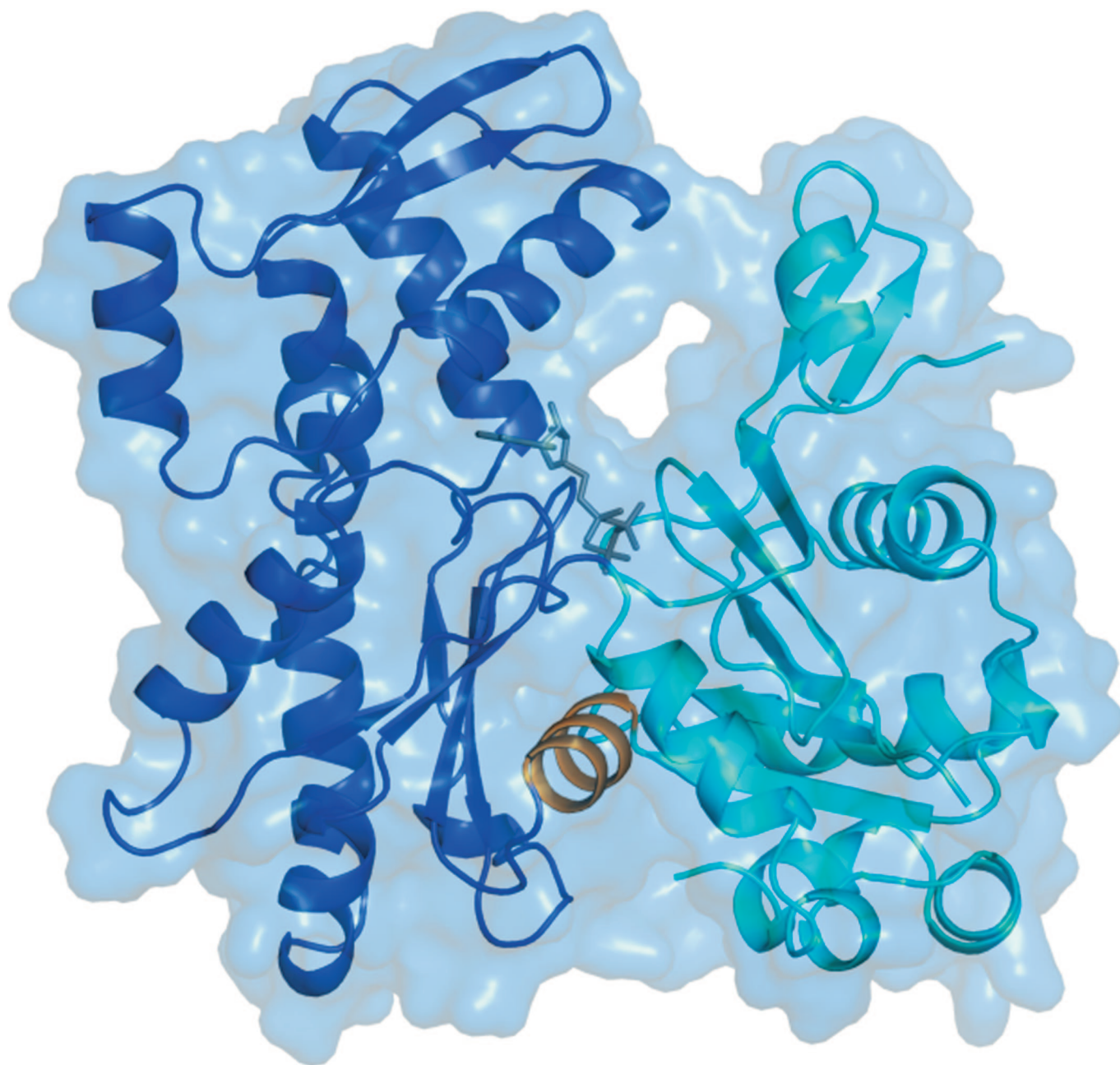
[Movie S1 \(MOV\)](#)



Movie S2. The binding of profilin to actin induces a moderate opening of the nucleotide cleft. The movie illustrates a linear interpolation between the atomic coordinates of the structures of profilin–*Dictyostelium*–actin and uncomplexed monomeric actin (1). Both a α -trace and a transparent surface representation are shown. Note that the structure of uncomplexed monomeric actin was selected for this comparison because it was obtained by mutagenesis in subdomain 4 and is thought to be free of perturbations resulting from the binding of an ABP or chemical cross-linking. Subdomain 3 and 4 of the structures were superimposed (blue) to highlight the relative movement of subdomains 1 and 2 (cyan). The magnitude of the rotation is 4.7° (see also Fig. 2A). Using the classical view of the actin structure as a reference, this rotation can be visualized as two perpendicular rotations of $\approx 3.3^\circ$. Although this movement appears less dramatic than previously anticipated (2, 3), it is probably sufficient to explain the stimulation of nucleotide exchange by profilin.

1. Rould MA, Wan Q, Joel PB, Lowey S, Trybus KM (2006) Crystal structures of expressed non-polymerizable monomeric actin in the ADP and ATP states. *J Biol Chem* 281:31909–31919.
2. Chik JK, Lindberg U, Schutt CE (1996) The structure of an open state of beta-actin at 2.65 Å resolution. *J Mol Biol* 263:607–623.
3. Schuler H (2001) ATPase activity and conformational changes in the regulation of actin. *Biochim Biophys Acta* 1549:137–147.

[Movie S2 \(MOV\)](#)



Movie S3. Opening of the nucleotide cleft is a unique feature of the protilin–actin structure. This movie was generated and colored as described for [Movie S2](#), but by interpolation between the structures of the complexes of protilin and G1 with unphosphorylated *Dictyostelium* actin. Comparison of the protilin–actin structures with virtually any other structure of actin in the protein databank, except for the wide-open structure of protilin– β -actin (1), results in a similar motion of the two major domains on each side of the nucleotide cleft relative to each other.

1. Chik JK, Lindberg U, Schutt CE (1996) The structure of an open state of beta-actin at 2.65 Å resolution. *J Mol Biol* 263:607–623.

[Movie S3 \(MOV\)](#)